

Doubly Fed Induction Generator Analysis Through Wavelet Technique

Bhola Jha^{1,*} and K.Ram Mohan Rao²

¹K.L.College of Engineering, Vaddeswaram-522502, Dept. of EEE, Andhra Pradesh, India.

²M.J College of Engineering and Technology, Hyderabad-500034, Dept. of EEE, Andhra Pradesh, India.

Received 17 November 2008; Revised 6 May 2009; Accepted 15 June 2009

Abstract

Because of the intermittent nature of wind, its integration to the power system is still promising with respect to power quality and stability. For the large penetration of wind energy, this paper using an embedded time-frequency localization features in wavelet, provides deep insight to the character of transient signals for a proposed test system comprising one thermal plant and three DFIG-based wind plants. The test system is first simulated and the results are mapped onto the wavelet format for accurate detection & better resolution of the characters of transients. This is found that the presence of lower frequency bandwidth signals accompanies relatively more energy and larger magnitude wavelet coefficients are the root cause for the stability and quality.

Keywords: DFIG, Wavelet, Time-Frequency Localization, Transients.

1. Introduction

Due to the increasing concern about the global warming, renewable energy systems especially wind energy generation have attracted great interests in the recent years. Large wind farms have been installed or planned around the world and the power ratings of the wind turbines are increasing. For many wind farms, wind turbines based on doubly fed induction generator technology are used.

In area of wind energy, limited numbers of wavelet-based research papers are reported [1] and [2]. CWT-based approach is proposed in [1] for the enhancement of damage detection of wind turbine blades. Wavelet-based ARMA model is presented in [2] for the short-term wind speed forecasting. For the large penetration of wind energy, an internationally recognized tool wavelet transform approach is proposed for the condition monitoring of the test system, comprises one thermal plant and three DFIG-based wind plants.

As analyzed from theory point of view, the wavelet can be formulated via a family of basis functions such that the signals can be described in a localized time and frequency format [3], [4] and [5]. Hence, by employing the long windows at low frequency and short windows at high frequencies, the wavelet transform will be capable of comprehending the time and frequency information simultaneously. For those transients in time-varying signals, they would be supervised more effectively, thereby encouraging the application of such method to enhance the detection capabilities.

This paper is organized in the sequences as follows: DFIG modeling is summarized in section 2. Overview of the test sys-

tem is described in section 3. Results of the test system are reflected in section 4. Paradigm of proposed wavelet-based approach is introduced in section 5. Results and discussions are presented in section 6. Conclusions are drawn in section 7.

2. Doubly – Fed Induction Generator Modeling

2.1 Configuration and Principles

The major component of the system is a wound rotor induction machine, which needs to excite at both the stator and rotor terminals. In variable speed drive applications, the so-called slip power recovery scheme is common practice. Power captured by the wind turbine is converted into electrical power by DFIG- based wind farm is shown in the Fig. (1). The generator assures efficient power production at variable speed [6]. The speed variability is made possible by directionally dependent transfer of slip power via converters. In sub synchronous speed the stator of DFIG feeds all the generating electrical power to the grid, and additionally makes slip/rotor power P_r available, which is fed, from converter to the rotor via slip rings. However in the super synchronous mode total power consists of the components fed by stator of DFIG plus rotor power P_r that is fed from the rotor to grid via converter. To obtain the sub and super synchronous speed operation the power converter of the rotor winding must be able to handle slip power in both directions using voltage source converters. Among the three power flow ports, i. e the stator terminals, rotor terminals and the rotor shaft, the rotor terminals acts as the regulating port, balancing the power flow of the entire system.

* E-mail address: bholaajhaeee@yahoo.co.in

The control system generates pitch angle, and the voltage command signal V_r & V_{gc} for C_{rotor} and C_{grid} respectively in order to control the power of wind turbine, DC voltage and voltage at grid terminals. C_{rotor} and C_{grid} have the capability for generating or absorbing reactive power and could be used to control the reactive power or the voltage at grid terminals. DC Link voltage is always constant for the bidirectional power flow.

The fundamental feature of the doubly fed induction generator is that the power processed by the converter is only a small fraction of total system power. Therefore, for large rating system it is possible to use a low rated high frequency switching PWM converter to achieve high performance, such as fast response, low harmonic distortion, high efficiency etc., without cost penalty.

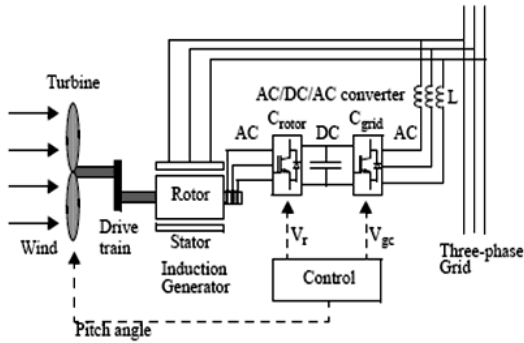


Figure 1. Doubly Fed Induction Generating System

2.2 Basic Equations for Modeling

The basic equations of the variable speed DFIG can be conveniently analyzed by classical rotating field theory with the well-known dq transformation [7]. For the rotor side controller the d-axis of the rotating reference used for d-q transformation is aligned with air gap flux.

$$V_{qs} = R_s I_{qs} + L_s p I_{qs} + \Omega_r \lambda_{ds} + L_m p I_{qr} \tag{1}$$

$$V_{ds} = R_s I_{ds} + L_s p I_{ds} + \Omega_r \lambda_{qs} + L_m p I_{dr} \tag{2}$$

$$V_{qr} = R_r I_{qr} + L_r p I_{qr} + L_m p I_{qs} \tag{3}$$

$$V_{dr} = R_r I_{dr} + L_r p I_{dr} + L_m p I_{ds} \tag{4}$$

Here,

$$\lambda_{dr} = L_r I_{dr} + L_m I_{ds} \tag{5}$$

$$\lambda_{qr} = L_r I_{qr} + L_m I_{qs} \tag{6}$$

$$\lambda_{qs} = L_s I_{qs} + L_m I_{qr} \tag{7}$$

$$\lambda_{ds} = L_s I_{ds} + L_m I_{dr} \tag{8}$$

Torque and Reactive Power in dq coordinate are given by

$$T_e = -\frac{3}{2} \frac{P}{2} (\lambda_{ds} I_{qs} - \lambda_{qs} I_{ds}) \tag{9}$$

$$Q = \frac{3}{2} (V_{qs} I_{ds} - V_{ds} I_{qs}) \tag{10}$$

Assuming the d-axis of the reference frame to be along with the air-gap flux,

$$\text{Implies, } \lambda_{qs} = 0 \tag{11}$$

Using (7), (9) and (11)

$$T_e = \frac{3}{2} \frac{P}{2} \frac{L_m}{L_s} \lambda_{ds} I_{qr} \tag{12}$$

Since, λ_{ds} remain unchanged. So, Torque/Active Power is controlled by q component of rotor current.

For λ_{ds} to be remain unchanged i.e. and using (1), (2), (7), (8), (10) and (11)

$$Q = \frac{3}{2} \Omega_r \lambda_{ds} I_{ds} \tag{13}$$

I_{ds} is a function of I_{dr} for a constant value of λ_{ds} .

Therefore, Reactive Power can be controlled by d component of rotor current.

3. Overview of Test System

The following figure (2) illustrates the test system based on [8], where 27 MW DFIG-Based wind farms is integrated to 500 MVA thermal power plant through 120 KM ring distribution feeder. Three Wind Power, each 9 MW at 575 V and One Thermal Power Plant at 22 KV are stepped up to Grid voltage of 120 KV through a step-up Transformer, 600 MVA, 22 KV/120 KV (delta-star). After integration, Total Harmonic Distortions (THD) is measured and eliminated (third and fifth order) by three phase harmonic filter having quality factor 20.

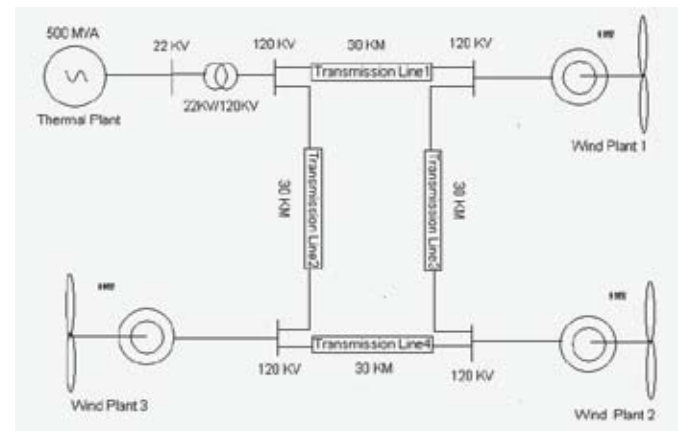


Figure 2. Test System

30 MVA load is applied on II transmission line distribution feeder whose parameters are mentioned in the appendix. L-G (Line to Ground) Fault is created near the wind power plant 2 for the duration 1.66 ms. A capacitor of 0.6 F is connected in between the rotor side converter and grid side converter. DC link voltage is

made almost constant at 1200 V for the bidirectional power flow in the rotor of DFIG. All the three wind farms are operating under three different slew rate, i. e the change in speed for the wind farm 1 is average, for wind farm 2 is more and wind farm 3 is less. This test system is simulated on MATLAB platform.

4. Results of the Test System

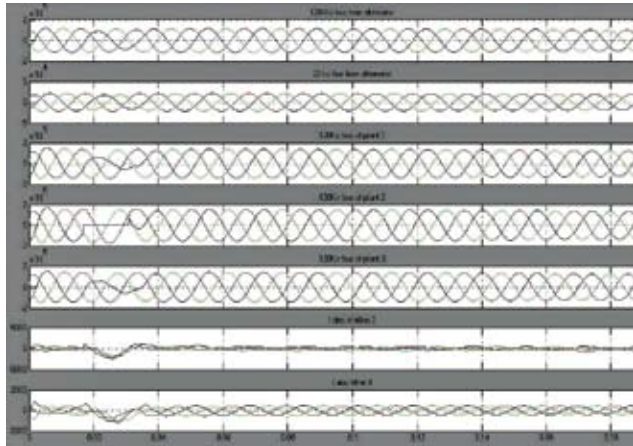


Figure 3. Thermal Plant

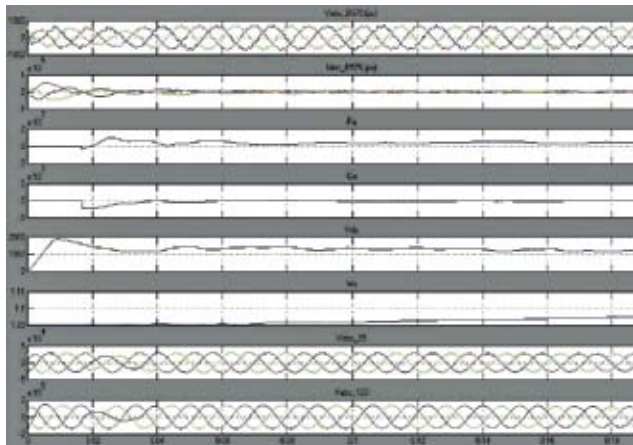


Figure 4. Wind Plant1

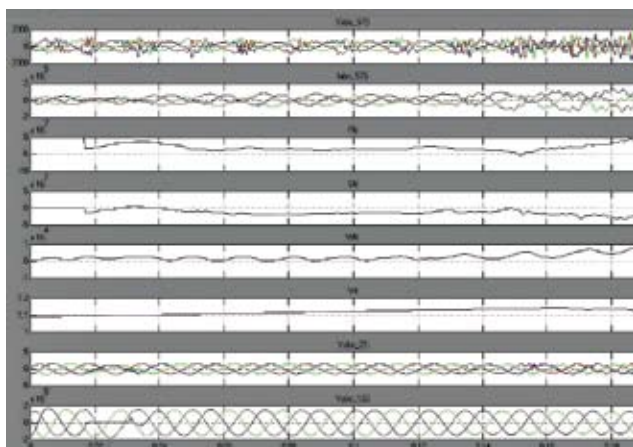


Figure 5. Wind Plant 2

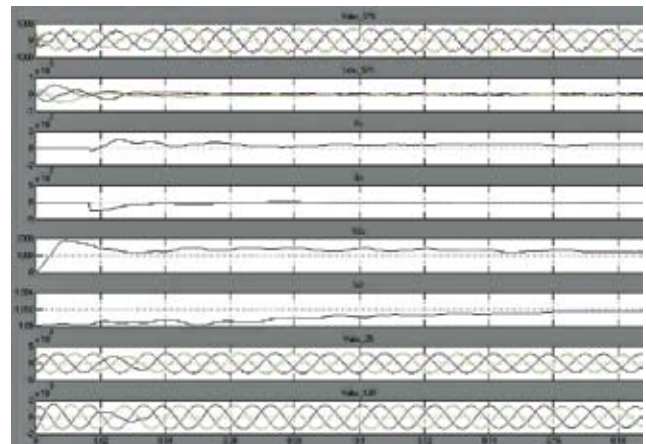


Figure 6. Wind Plant 3

The results of the test systems like bus voltages, active power, reactive power, DC link voltage etc. for wind plants as well as thermal plant are presented in figures (3), (4), (5) and (6). Almost constant DC link voltage and zero reactive power validate the test system. The transients in waveforms at the starting are seen due to the change in rotor power for restoring the DC link voltage.

5. Wavelet Analysis

The ability to provide variable time-frequency resolution is hallmarks of wavelet transform. Wavelet transform is relatively new mathematical technique, which is used to analyze signal in nature. It is becoming the focus point of much science, and is fondly delighted tool by scientists. It plays a very important role in signal and information processing.

5.1 Discrete Wavelet Transform (DWT)

The wavelet transformation is processes of determining how well a series of wavelet functions represent the signal being analyzed. The goodness of fitting of the function to the signal is described by the wavelet coefficients. The result is a bank of coefficients associated with two independent variables, dilation and translation. Translation typically represents time, while scale is a way of viewing the frequency content. Larger scale corresponds to lower frequency meaning thereby better resolution. The most efficient and compact form of the wavelet analysis is accomplished by the decomposing a signal into a subset of translated and dilated parent wavelets, where these various scales and shifts in the parent wavelet are related based on powers of two. Full representation of a signal can be achieved using a vector coefficients the same length as the original signal.

Considering a signal consisting of 2^M data points, where M is an integer. DWT requires 2^M wavelet coefficients to fully describe the signal. DWT decomposes the signal into $M+1$ levels, where the level is denoted as j and the levels are numbered $i = -1, 0, 1, 2, 3 \dots M-1$. Each level i consists of $j = 2^i$ wavelet translated and equally spaced 2^{M-j} intervals apart.

The $j = 2^i$ wavelets at level i are dilated such that an indi-

vidual wavelet spans N-1 of that level interval, where N is the order of wavelet being applied. Each of the $j = 2^i$ wavelets at level i is scaled by a coefficient $a_{i,j}$ determined by the convolution of the signal with the wavelet. Notation is such that i corresponds to wavelet dilation and j is the wavelet translation in level i .

The forward wavelet transform determines the wavelet coefficients $a_{i,j}$ of j wavelet at each level i . For the signal $f(n)$, the DWT is

$$a_{i,j} = a_{2^i+j} = \sum_n f(n) \psi_{i,j}(n) \tag{14}$$

Here, ψ is mother wavelet.

5.2 Continuous Wavelet Transform (CWT)

While the DWT is most efficient and compact, its power of two relationships the scale fixes its frequency resolution. Often it is desired to differentiate between smaller frequency bands than DWT allows. This is possible by using scales that are more closely spaced together than the 2^i relationship, and is the basis for the Continuous Wavelet Transform (CWT).

For a signal $f(t)$, CWT determines the coefficients as

$$a(i, j) = \int_{-\infty}^{+\infty} f(t) \psi(i, j, t) dt \tag{15}$$

Here, ψ is mother wavelet

The number of coefficients necessary to describe the signal may be larger than the signal strength, as the CWT over samples the signal.

5.3 Scalogram

In this paper the wavelet coefficients is used to provide the scalogram, which describes the signal energy on time-scale domain. This facilitates identification of time varying energy flux spectral evolution and transient bursts not readily discernible using time or frequency domain method

In this paper, Daubechies wavelet is applied in one-dimensional CWT for scalogram, which reveals much information about the nature of non-stationary processes that was hidden. Scalogram is useful for the diagnosis of special events in the structural behavior. Any change in frequency content e.g. initiation of stiffness degradation can easily be identified by the scalogram.

Scalogram is a plot of coefficients on time-scale plane. Each point on this plane represents wavelet coefficients. The wavelet coefficients are well suited for analyzing non-stationary events such as transient and evolutionary phenomena. There are 2^i coefficients to describe the energy at the i^{th} frequency band, for $i = 0, 1, 2, \dots, M-1$ where the signal consists of 2^M data points. The coefficients in a particular band represent the energy at that interval equally spaced over the duration of the signal. When the squared coefficients are plotted on a time-scale grid, the transfer of energy from one band to next would be observed along the time scale. This is called the scalogram.

6. Results and Discussion

In this paper, the signal consists 10286 data points whereas the coefficients generated at the eight levels are 10323. This happens because the CWT over samples the signal and so wavelet coefficients contain partial redundancies of information.

Line-Ground fault occurs on the ring distribution feeder near by the wind plant 2 is clearly detected, can be seen in figure (8). Discrete Wavelet Transform (DWT) is used to decompose the fault signal at d1 (low frequency) level for intensifying the high frequency oscillations present at the instant of fault, shown in figure (7). These oscillations are divided into eight frequencies bandwidth i.e. the scalogram format to extract the root cause.



Figure 7. Presence of oscillations

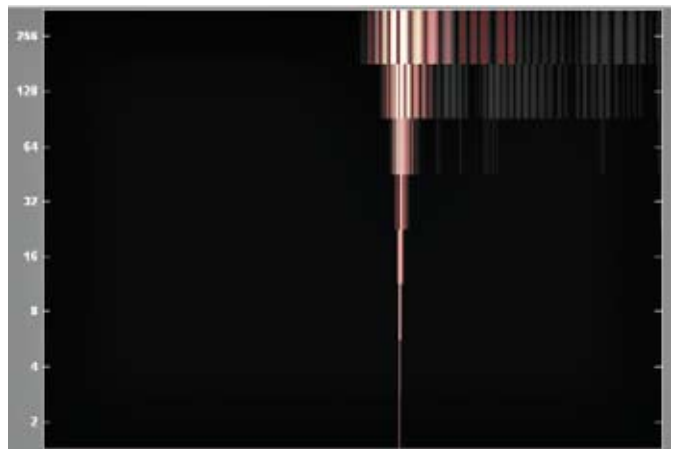


Figure 8. Scalogram

Horizontal axis represents time whereas vertical axis, scale increasing from bottom to top. Higher scale corresponds to low frequency. Volume bounded by the surface decreases from upper frequency to lower frequency band. Therefore the energy strength of the faulty signal decreases towards lower frequency i.e. higher frequency bandwidth. This is clearly observed in figure (8). Transfer of energy for a particular band is also clearly seen, which is more in the upper frequency band i.e. low frequency bandwidth. Low frequency bandwidth signal carries more energy and persists relatively for a longer duration on the system.

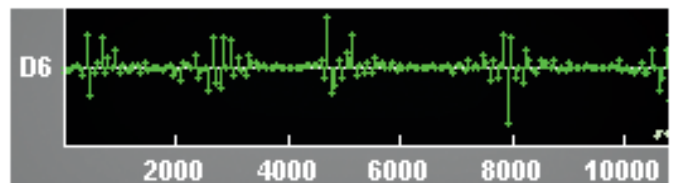


Figure 9. Grid coefficients before fault

Wavelet coefficients for the grid are generated under faulty and healthy conditions for clear discriminating the wind-thermal integration. These data are plotted through wavelet coefficients

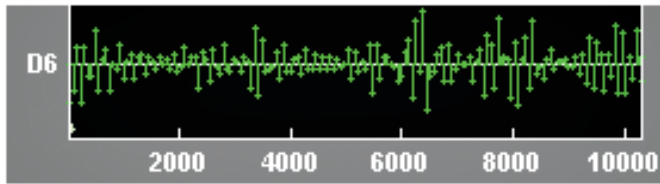


Figure 10. Grid coefficients after fault

selection 1-D, which are shown in figure (9) and (10). As having better resolution, only D6 level coefficients are presented here. The occurrence of larger magnitude coefficients in the wavelet domain is the identification the impulsive events.

7. Conclusion

Impacts of wind-thermal integration and L-G fault are exhibited through wavelet coefficients and scalogram. The presence of low-frequency bandwidth signals carries more energy and persists

relatively for a longer duration on the system is the root cause for the stability and quality of the system. The occurrence of larger magnitude wavelet coefficients is the identification of impulsive response. Special events or change in frequency or stiffness degradation is diagonalized.

8. Future Extension

For the large wind energy penetration, development of an effective filter/controller to diminish the transients for the enhancement of quality and stability of the system.

Acknowledgement

Authors are very much thankful to Mr. G. Vinay Kumar, R. Avinash, V. Manoj Kumar, D. Satyanarayana Raju and G. Sharath Veer for extending their cooperation in simulation of the test system.

References

- Chin-Shun Tsai, Cheng-Tao Hsieh, and Shyh-Jier Huang "Enhancement of Damage-Detection of Wind Turbine Blades Via CWT-Based Approaches" IEEE transactions on Energy Conversion, Vol. 21, No. 3, Sept. 2006. pp 776-781.
- CAO Lei and LI ran "Short-Term Wind Speed Forecasting Model for Wind Farm Based on Wavelet Decomposition" DRPT 2008, 6-9 April, Nanjing China. pp 2525-2529.
- "Wavelet Transforms" by Rghuveer. M. Rao and Ajit. S. Bopardikar Pearson Education, Low Price Edition, 2005.
- Wavelet Tutorial Vol. I, II, III by Robi Polikar.
- www.mathworks.com
- Rajib Datta and V.T. Ranganathan "Variable Speed Wind Power Generation Using Doubly-Fe Wound Rotor Induction Machine-A comparison with Alternative Schemes" IEEE transactions on energy conversion, vol. 17, No.3, September 2002.
- P.C. Kraus, O. Wasynczuk, Scott. D. Sudhoff, Analysis of Electric Machinery, 2nd Edition, 2004, John Wiley and Sons.
- Changling Luo and Boon-Teck "Frequency Deviation of Thermal Power Plants Due to Wind Farms" IEEE Transactions on Energy Conversion, Vol. 21, No. 3, Sept. 2006. pp 708-716.

Appendix

II - Transmission Line Parameter

Parameters	Positive Sequence	Zero Sequence
Resistance	0.00273Ω/KM	0.1864Ω/KM
Inductance	0.9337mH/KM	4.1264mH/KM
Capacitance	12.74nF/KM	7.751nF/KM

Doubly Fed Induction Generator Parameter

S.N	Parameter	Values
1	Capacity	9 MW
2	Voltage	575 V
3	No. of Poles	6
4	Power Factor	0.9
5	Inertia Constant	5.04
6	Stator Resistance (in per unit)	0.00706
7	Stator Inductance (in per unit)	0.171
8	Rotor Resistance (in per unit)	0.005
9	Rotor Inductance (in per unit)	0.156
10	Magnetizing Inductance (in per unit)	2.9